3D Transient Calculation of an Induction Machine with Squirrel-Cage Rotor

C. Schlensok and G. Henneberger
Department of Electrical Machines (IEM),
Aachen University (RWTH Aachen)
Schinkelstraße 4
D-52064 Aachen, Germany
e-mail: christoph.schlensok@iem.rwth-aachen.de

C. Kaehler
Bosch Rexroth AG
Department for Electric Drives and Controls
Bgm.-Dr.-Nebel-Straße 2
D-97816 Lohr, Germany
e-mail: christian.kaehler@boschrexroth.de

Abstract

The numerical simulation of induction machines with squirrel-cage rotor using the Finite-Element Method (FEM) requires a transient solution process. In order to save computation time, the calculations are usually performed applying 2D models. However, with this approach the skewing of the rotor cannot be considered. Therefore, the 2D principle of virtual skewing is applied. The induction machine is computed employing a transient 2D model. From the results of this calculation the rotor-bar currents are derived. After this step five slices of the machine are modeled rotating the rotor in each slice for one fifth of the skewing. Using the original stator currents and the derived rotor-bar currents as excitation, these five magneto-static models are computed rotating the rotor in each time step. This paper presents the calculation of an induction machine with squirrel-cage rotor avoiding the described detour of first deriving the rotor-bar currents and then performing magneto-static calculations. Here, the machine is directly calculated by using a 3D transient solver.

Formulations for 2D and 3D A-Approaches

The finite-element formulations used in 2D and 3D both use an A-approach and are part of the object-oriented solver package *i*MOOSE [1] developed at the IEM. The transient FEM formulation for the 2D solver takes the rotational movement into account. It is node-based and reads:

$$\int_\Gamma \left(\nabla \cdot \alpha_i \cdot \nu \cdot \nabla \cdot A_z(t) + \alpha_i \cdot \sigma \cdot \frac{\partial}{\partial t} A_z(t) \right) \mathrm{d}\Gamma = \int_\Gamma \left(\alpha_i \cdot J_{z0}(t) \right) \mathrm{d}\Gamma. \tag{1}$$

The equation given in Galerkin formulation [2] has to be solved in the entire model region Γ. The material parameters ν and σ represent the non-linear reluctivity and the linear conductivity. The shape function of an element is defined by α_i. Triangular shaped elements are used. $J_{z0}(t)$ describes the z-component of the given coil current-density as the only type of excitation.

The 3D solver is edge-based and applies the magnetic vector potential A in all regions Γ as well:

$$\int_\Gamma \left(\nabla \times \overset{\circ}{\alpha}_i \cdot \nu \cdot \nabla \times \overset{\circ}{A}(t) + \overset{\circ}{\alpha}_i \cdot \sigma \cdot \frac{\partial}{\partial t} \overset{\circ}{A}(t) \right) \mathrm{d}\Gamma = \int_\Gamma \left(\overset{\circ}{\alpha}_i \cdot \overset{\circ}{J}_0(t)\big|_{\sigma=0} \right) \mathrm{d}\Gamma. \tag{2}$$

α_i defines the shape function of the 3D edge elements. ν and σ are again the non-linear reluctivity and the linear conductivity, respectively. $J_0(t)$ is the given coil current density. For the linear interpolation of the time-dependent variables of both solvers 2D and 3D the first order time-step algorithm is applied and $A(t)$ can be written as a function of time as follows:

$$A(t) = (1-\Theta) A_n + \Theta \cdot A_{n+1} \tag{3}$$

$$\Theta = \frac{t - t_n}{t_{n+1} - t_n} = \frac{t - t_n}{\Delta t}; \quad 0 \le \Theta \le 1. \tag{4}$$

Θ is the weighting parameter and is set to $\Theta = 2/3$ according to the Galerkin scheme [3]. The two transient solvers use different methods for the rotation of the mesh, i.e. the rotor mesh. In the case of the 2-dimensional solver the air gap is divided into three layers. Both outer layers are attached to the

rotor and stator mesh, respectively. The center layer is the rotating air gap and remeshed in each time step. In this way any arbitrary time step, i.e. stepping angle, can be applied. In order to avoid the time consuming 3-dimensional remeshing the 3D solver applies the lock-step method for the rotation. Therefore, the mesh of the air gap must be meshed equidistantly at the boundary layer which must consist of a double node layer. The movement is now performed virtually by using the nodes of the double node layer and sliding a boundary condition from step to step. This way the mesh is kept stationary. Thus, the flux is coupled between virtually moving and stationary regions [4].

Finite-Element Models of the Induction Machine with Squirrel-Cage Rotor

The induction machine studied in this paper holds N_S = 36 stator and N_R = 24 rotor slots. The two-layer and three-phase winding has 4 poles. Therefore, it is possible and sufficient to only model a quarter of the geometry for the electro-magnetic field simulation. The finite-element models of both, 2D and 3D case, consist of the rotor and stator laminations and windings. It is necessary to model the air between rotor and stator, i.e. the air gap as well as the surrounding air of the machine. In both models the rotor bars are labeled as eddy-current regions. The short-circuit rings of the 3D model are assigned as eddy-current regions as well. The stator and rotor laminations of both models are simulated with non-linear ferromagnetic material properties.

The 2-dimensional model, depicted in Fig. 1(a), consists of 5.786 first order triangular elements and 2.944 nodes. The 3-dimensional model (Fig. 1(b)) consists of 189.740 first order tetrahedral elements with 38.187 nodes. In Fig. 1(b) the two-layer winding is marked in different colors. Since three neighboring slots hold the same phases these three phases can be labeled with one material as done for the 2D model in Fig. 1(a). In the case of 2-dimensional simulation three current-density data files are read in each time step for the three coil labels. The 3-dimensional case affords current excitation due to the inhomogeneous meshing of the stator bars. The bars are not evenly meshed in axial direction so that a current-density vector could possible have a component on single surface elements of the bars which point through the surface. This would hurt the condition of $\nabla \cdot B = 0$.

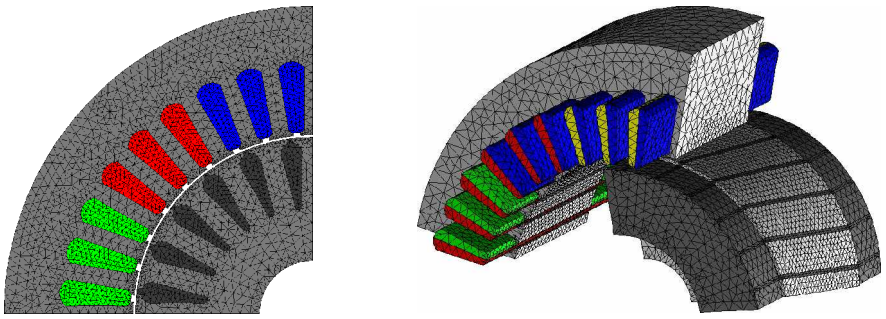

(a) 2-dimensional FE Model. (b) 3-dimensional FE Model.

Figure 1. Finite-Element Models of the Induction Machine with Squirrel-Cage Rotor for 2D (a) and 3D (b) Simulation.

The simulations both provide next to the flux-density distribution of each time step the torque of the machine and the net force acting onto the rotor. Because the models only consist of a quarter of the entire machine the radial components in x- and y-direction of the net force cannot be analyzed reasonably. Therefore, only the axial component in z-direction of the 3-dimensional simulation is regarded. The 2D simulation of course inherently cannot provide an axial component.

Specification of the Simulations

The computation time of the 2D simulation is less critical than in the 3D case. The time step is reduced by 50 % compared to the time step in the 3D simulation. Therefore, twice as much time steps have to be calculated in 2D when compared to the 3D model to reach the same real time. The locked step width of the 3D simulation is set to $\alpha = 2^{\circ}$. This results in a time step of $t_{3D} = 250\mu s$ for the stator frequency at $f = 50Hz$. The rotor speed is $n = 1333.\overline{3}\,\mathrm{min}^{-1} = 22.\overline{2}Hz$, which results in a slip of $s = 11.\overline{1}\%$. The excitation currents are assumed to be sinusoidal for both cases.

Results of Torque and Force

Fig. 2(a) and 2(b) show the time-dependent torque behavior for the 2- and 3-dimensional simulation, respectively. Both show a transient phenomenon since the currents as well as the speed are "switched on" in the simulation at $t = 0$. The magnetic field has to be build up. After the transient phenomenon has died out the simulation is in a steady state and the torque behavior can be analyzed.

The torque of the 2D simulation shows a strong but even oscillation with the maximum peak-to-peak value of $\Delta T_{3D} = 1.67\,Nm$. In the case of the 3D torque there is a very significant fundamental oscillation with $\Delta T_{2D} = 0.445\,Nm$. The average torque values diverge as well: $T_{2D} = 3.81\,Nm$ and $T_{3D} = 2.89\,Nm$. This may be the result of the 3-dimensional effects not regarded in the 2D simulation, i.e. the skewing of the rotor and the front leakage.

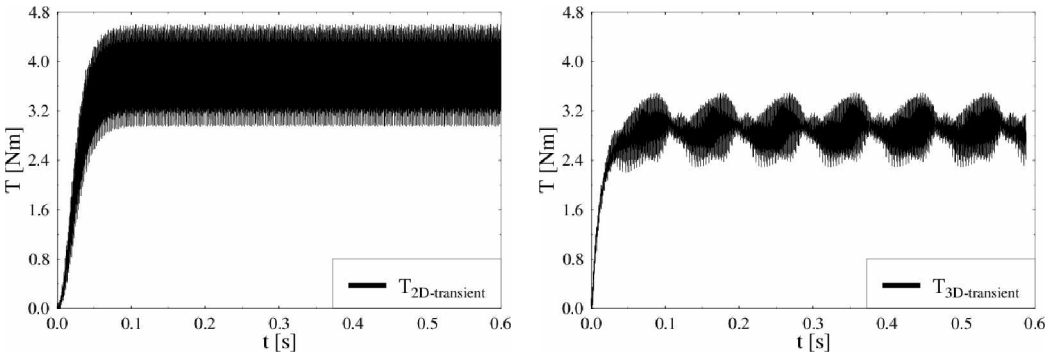

(a) 2D Time-Dependent Torque-Behavior. (b) 3D Time-Dependent Torque-Behavior.

Figure 2. Time-Dependent Torque-Behavior for 2D (a) and 3D (b) Simulation.

In a second step the torque behavior is analyzed in the frequency domain using the Fast-Fourier Transformation (FFT) [5]. Both signals the time-dependent torque-behavior of the 2D and the 3D simulation are transformed. Fig. 3 shows the results. The cut-off frequency of the 2D simulation is twice as high as in the case of the 3D simulation due to the smaller time step.

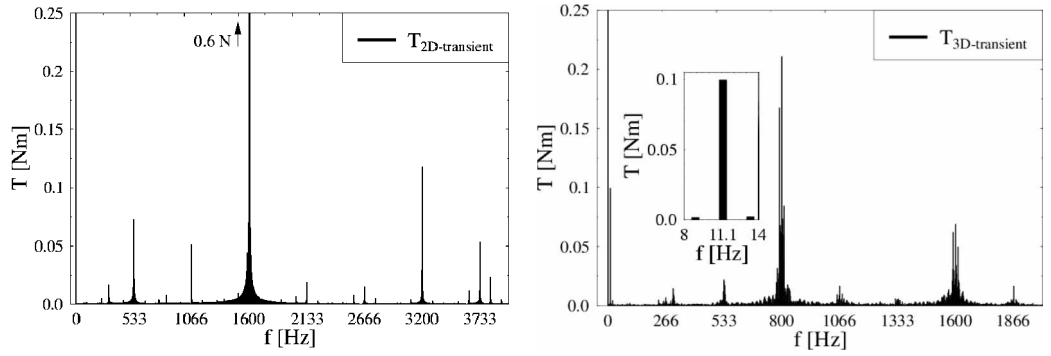

(a) 2D Torque-Behavior in the Frequency Domain. (b) 3D Torque-Behavior in the Frequency Domain.

Figure 3. Torque-Behavior in the Frequency Domain for 2D (a) and 3D (b) Simulation.

The two resulting spectra differ strongly from each other. Although the peaks appear at the same frequencies (266.66 Hz and higher harmonics) their amplitudes are significantly different. The only harmonic order not appearing in the 2D spectrum but in the 3D spectrum is the double slip frequency $2 \cdot f_s = 11.1\,Hz$ which is shown in Fig. 3(b) in the detail frame. This harmonic order is the fundamental frequency for the time-dependent torque signal shown in Fig. 2(b). One reason for this significant difference between the two signals is the rather coarse meshing in the 3-dimensional FE model. Because of the lock-step method the mesh is not changed in every time step. This can cause oscillations. In the case of the 2D-FE simulation the mesh is changed in each time step in the center air-gap layer which prevents the signal from oscillating.

The other differences between the two spectra derive from aliasing effects [6]. All harmonic orders are multiples of the rotor and stator frequency $f_R = 22.2\ Hz$ and $f_S = 50\ Hz$. The highest harmonic orders are multiples of the rotor and stator slot harmonics of the rotor frequency $n \cdot 24 \cdot f_R = n \cdot 533.3\ Hz$ and $n \cdot 36 \cdot f_R = n \cdot 800\ Hz$. With *n* being the harmonic order. This results in a very high peak for 1,600 Hz in the spectrum of the 2D simulation (Fig. 3(a)). The highest peak in the spectrum of the 3D simulation is at 800 Hz (Fig. 3(b)). Looking at the spectrum in Fig. 3(a) again one can see that this peak is the aliasing frequency $f_{alias} = 3200\ Hz$ "mirrored" at the cut-off frequency of the spectrum in Fig. 3(b) at $f_{cut-off,3D} = 2000\ Hz$. This means that the spectrum of the 3D simulation is not reliable. The sampling (time step of the simulation) is too coarse.

Fig. 4 shows the same analysis for the axial force component of the net force for the 3D simulation. The spectrum is very similar to the torque spectrum in case of the 3D simulation in Fig. 3(b). The axial net-froce component itself pulsates very strongly with twice the slip frequency as the torque does. The same alias frequency can be detected. The average Lorentz force is $F_z = -39.37\ N$.

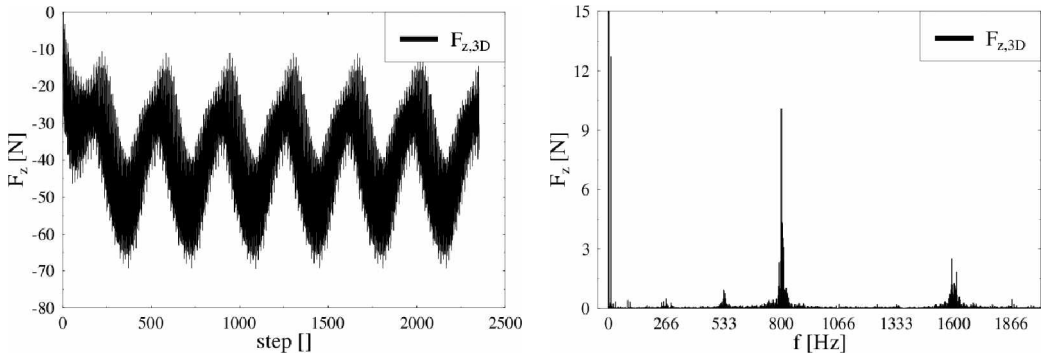

(a) 3D Force-Behavior in the Time Domain. (b) 3D Force-Behavior in the Frequency Domain.

Figure 4. Axial Force-Behavior in Time (a) and Frequency Domain (b) 3D Simulation.

Conclusion

In this paper the results of a 2D and a 3D transient electro-magnetic FEM simulations of an induction machine with squirrel-cage rotor are compared. Both solvers using the A-approach provide the torque and the components of the net force acting on the rotor. The results show, that there are some difficulties to be managed using 3D computation for and induction motor. Depending on the point of operation the constant time step Δt is very important for the reliability of the spectra. The results of the regarded simulations show aliasing effects in the 3D spectra for torque and net force.

Due to the chance of misinterpretation of the results and the very long computation times – 5 days (2D) compared to 7 weeks (3D) – the 3D simulation is not very reasonable yet. Another problem is the discretization of the geometry which leads to oscillations of the results if it is too poor.

REFERENCES

1. G. Arians, T. Bauer, C. Kaehler, W. Mai, C. Monzel, D. van Riesen, and C. Schlensok, "Innovative Modern Object-Oriented Solver Environment – *i*MOOSE," *Available: http://www.imoose.de*.
2. G. Arians, G. Henneberger, "Object-oriented analysis and design of transient finite-element solvers applied to coupled problems," in *9th Conference on Electromagnetic Field Computation*, Milwaukee, USA, CEFC 2000.
3. O. C. Zienkiewicz, R. L. Taylor, *The finite-element method*, London, McGraw-Hill Book Company, 1989, pp. 346-361.
4. C. Kaehler, G. Henneberger, "Eddy-current computation in the claws of a synchronous claw-pole alternator in generator mode," *IEEE Transactions on Magnetics 38*, IEEE Magnetics Society, 2002, pp. 1201-1204.
5. I. N. Bronstein, K. A. Semendjajew, *Taschenbuch der Mathematik*, 25. Auflage, Stuttgart Leipzig, B. G. Teubner Verlagsgesellschaft, 1991, pp. 616-618.
6. H. D. Lüke, *Signalübertragung*, 7. Auflage, Berlin Heidelberg New York, Springer-Verlag, 1999.